by indirect methods. In all of these cases there were serious differences in the values of $k_{cat.}$ of up to several orders of magnitude.[29,31,32]

Therefore we believe that these indirect methods are not reliable, and direct methods of observing superoxide dismutase activity are to be preferred whenever possible.

Conclusion

We have demonstrated that $(op)_2Cu^{2+}$ is a good catalyst for superoxide dismutation with a "turnover" rate constant of $k_{cat.} = (5.1 \pm 0.9) \times 10^8\ M^{-1}\ s^{-1}$, a value that is only six times lower than that of SOD.

We have determined, for the first time, the reaction mechanism of the oxidation of $(op)_2Cu^+$ by molecular oxygen in aqueous solution, a mechanism that proceeds via a superoxide intermediate. The redox potential of the $(op)_2Cu^{2+}$ complex was determined to be $E^\circ_{(op)_2Cu^{2+}/(op)_2Cu^+} = -0.055$ V.

The biological damage of DNA in the presence of $(op)_2Cu^{2+}$ has been interpreted to be due to OH, being formed in reaction 22. In some of the studies published, there was not sufficient excess of H_2O_2 over O_2 to assure that most of the $(op)_2Cu^+$ will react with H_2O_2 and yield OH.[11,12,14] Therefore we conclude that $(op)_2Cu^+$ is possibly bound to DNA, and that the rate constants of relevant reactions of free and bound $(op)_2Cu^+$ may be different.

The binding of metal ions or their complexes to biological targets may change the chemical properties of the metal ion. The bound metal ion may play a large role, in both toxic[33] and pharmacological mechanisms.[33] The metal binding may also serve as a site-specific or site-directing mechanism.[34,35]

Acknowledgment. We wish to thank Prof. D. Meyerstein for valuable comments. This work was supported by DOE under contract DE-AC02-76EV03221 and by Grant No. 1409 of the Council of Tobacco Research.

Registry No. $(OP)_2Cu^+$, 17378-82-4; $(OP)_2Cu^{2+}$, 15823-71-9; O_2^-, 11062-77-4; H_2O_2, 7722-84-1.

---

(31) E. Lengfelder and U. Weser, *Bull. Eur. Physiopath. Respir.*, **17**, 73 (1981).

(32) C. Bull, J. A. Fee, P. O'Neill, and E. M. Fielden, *Arch. Biochem. Biophys.*, **215**, 551 (1982).

(33) J. R. J. Sorenson, "Inflammatory Diseases and Copper", Humana Press, New Jersey, 1982.

(34) N. R. Bachur, S. L. Gordon, and M. V. Gee, *Cancer Res.*, **38**, 1745 (1978).

(35) W. Bors, M. Saran, and G. Czapski, In "Biological and Clinical Aspects of Superoxide and SOD", W. H. Bannister and J. V. Bannister, Eds., Elsevier/North Holland, 1980, pp 1-31.

Effects of Secondary Bonding Interactions on the $[Fe_4S_4]^{2+}$ Core of Ferredoxin Site Analogues: $[Fe_4S_4(SC_6H_4\text{-}o\text{-}OH)_4]^{2-}$, a Distorted Cubane-Type Cluster with One Five-Coordinate Iron Atom

R. E. Johnson,[1a] **G. C. Papaefthymiou,**[1b] **R. B. Frankel,**[1b] **and R. H. Holm***[1a]

Contribution from the Department of Chemistry, Harvard University, Cambridge, Massachusetts 02138, and the Francis Bitter National Magnet Laboratory, Massachusetts Institute of Technology, Cambridge, Massachusetts 02139. Received May 16, 1983

Abstract: The series $[Fe_4S_4(SC_6H_4\text{-}o\text{-}X)_4]^{2-}$ with X = NH_2 (**1**), OMe (**2**), OH (**3**), and SMe (**4**) was prepared in order to examine the possible formation of five-coordinate Fe sites in cubane-type clusters with the biologically significant $[Fe_4S_4]^{2+}$ core oxidation level. The compound $(Et_4N)_2(\mathbf{3})$ crystallizes in monoclinic space group $P2_1/c$ with $a = 11.786$ (3) Å, $b = 20.701$ (6) Å, $c = 20.536$ (7) Å, $\beta = 94.42$ (2)° and $Z = 4$. The cluster contains three conventional tetrahedral FeS_4 sites and one distorted trigonal-bipyramidal FeS_4O site, in which the $o\text{-}HOC_6H_4S^-$ ligand forms a chelate ring with the bond distances Fe–S = 2.313 (3) Å and Fe–O(H) = 2.318 (5) Å. The former bond, being only 0.035 Å longer than the mean of three other terminal Fe–S distances, represents a primary interaction; the Fe–OH bond distance reflects a weaker, secondary interaction. In the solid state the ^{57}Fe Mössbauer spectrum of **1** is a single quadrupole doublet, indicative of no bonding interactions with the NH_2 group. The spectrum of **3** consists of three doublets with a 1:2:1 intensity ratio, one of which has an unusually large isomer shift ($\delta = 0.51$ mm/s at 4.2 K relative to Fe metal at this temperature). The spectrum of **4** was fit with two doublets in a 1:1 ratio; one of these has $\delta = 0.54$ mm/s. On the basis of the structure of **3** the high velocity doublets are assigned to five-coordinate Fe atoms; parameters of the remaining doublets are usual for conventional $[Fe_4S_4(SR)_4]^{2-}$ clusters with tetrahedral FeS_4 sites. The spectrum of **2** is suggestive of very weak secondary interactions. Absorption spectral data and redox potentials are reported for **1**–**4** and para-substituted analogues of **1**–**3** in DMF solutions. On the basis of property comparisons with $[Fe_4S_4(SR)_4]^{2-}$ (R = Ph, $p\text{-}C_6H_4OH$), the high-energy charge-transfer band (440 nm) and anodically shifted potentials of cluster **3** are considered to result from O–H··S intraligand hydrogen bonding. The Mössbauer spectrum of **3** reveals that Fe–OH interactions are largely absent in frozen acetonitrile solution. Hence it is probable that secondary interactions are imposed properties of the crystalline state. The isomer shifts of doublets in the spectra of **3**, **4**, and the recently reported $[Fe_4S_4(SPh)_2(S_2CNEt_2)_2]^{2-}$ (having two five-coordinate sites) are the largest known for clusters with the 2+ core and are very similar to those (0.52–0.57 mm/s) of the P clusters of nitrogenase. The structural feature of five-coordination and associated secondary interactions are appropriate inclusions in formulations, and approaches to synthetic representations, of P clusters. At present this feature is the only known means of placing δ values of $[Fe_4S_4]^{2+}$ clusters in the range of the spectroscopically unique P clusters.

The chemistry of the cubane-type clusters $[Fe_4S_4(SR)_4]^{2-,3-}$ has been extensively developed, and the role of these clusters as structural and electronic analogues of oxidized (**1**) and reduced (**2**) ferredoxin protein sites has been demonstrated.[2-7] Among the leading properties of these clusters are reversible electron-transfer reactions, delocalized electronic structures with anti-

---

(1) (a) Harvard University. (b) M.I.T.

(2) Holm, R. H. *Acc. Chem. Res.* **1977**, *10*, 427.

(3) Holm, R. H.; Ibers, J. A. In "Iron-Sulfur Proteins"; Lovenberg, W., Ed.; Academic Press: New York, 1977; Vol. III, Chapter 7.

0002-7863/83/1505-7280$01.50/0

ferromagnetically coupled Fe atoms, and compressed tetragonal (**1**) and nonuniform (**2**) distortions of the Fe_4S_4 cores in the solid state from idealized T_d symmetry. This structural aspect of **1**, although variable in extent, is a consistent feature of some five clusters,[4,7,8] whose detailed stereochemistry has been compared and analyzed.[4,7] Isoelectronic protein clusters exhibit the same type of distortion of the $[Fe_4S_4]^{2+}$ core[9,10] and magnetic and spectral properties that are very similar from one protein to another[11] and to their analogues **1**. The same comment applies to protein $[Fe_4S_4]^{+}$ sites and their analogues **2** in solution.

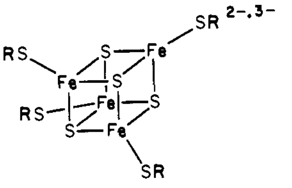

1 (2−) 2 (3−)

Whereas there is substantial uniformity in the properties of $[Fe_4S_4]^{2+,1+}$ protein[10,11] and analogue[4–7,12] clusters, it is apparent that there is at least one other type of native tetranuclear cluster that is significantly different from these. Here reference is made to the "P clusters" of nitrogenase, whose properties have been reviewed.[14,15] Chemical (core extrusion[16]) and Mössbauer spectral[17,18] evidence are supportive of the presence of ~4 Fe_4S_4-type clusters. Distinctive properties of these clusters include ^{57}Fe isomer shifts of the protein as isolated suggestive of a strongly reduced core, the absence of an EPR signal of the protein either as isolated or when oxidized by one electron (ground state $S \geq {}^{5}/_{2}$[17b,19a]), and MCD spectra atypical of conventional $Fe_4S_4(S\text{-}Cys)_4$ clusters with any of the core oxidation levels $[Fe_4S_4]^{3+,2+,1+}$.[19] In addition, Mössbauer results[17,18] reveal a 3:1 population of Fe atoms (D, Fe^{2+}) in diamagnetic clusters of the isolated protein, with the unique Fe atom (Fe^{2+}) having a quadrupole splitting typical of a high-spin tetrahedral $Fe^{II}–S_4$ site. The collective properties of P clusters are highly suggestive of these being variants of the more usual protein and analogue Fe_4S_4 clusters, but neither the nature of the variation(s) nor the core oxidation levels are known. In particular, the oxidation level/isomer shift linear correlation established for analogue complexes[20] and applicable to proteins does not hold unless, at the least, P clusters contain tetrahedral FeS_4 sites.

Attention has been directed to the possibility that P-cluster variations may include one or more terminal ligands other than cysteinate and some or all Fe atoms that are not four-coordinate.[14,15,21] Recently, $[Fe_4S_4(OPh)_4]^{2-}$[21] and $[Fe_4S_4(SPh)_2(Et_2dtc)_2]^{2-}$[22] have been prepared and characterized for the purpose of ascertaining the effects of ligand and structural variations on $[Fe_4S_4]^{2+}$ core properties. The latter cluster contains two five-coordinate Fe atoms. Earlier the species $[Fe_4S_4X_4]^{2-}$ (X = Cl, Br, I) had been isolated[23] and $[Fe_4S_4(SR)_{4-n}(OAc)_n]^{2-}$ (n = 1–4) generated in solution.[24] We have been attracted to the possibility that additional bonding interactions, involving physiological-type ligands and affording one or more five-coordinate Fe atoms, may impose significant structural and electronic variations compared to the well-studied $[Fe_4S_4(SR)_4]^{2-,3-}$ clusters. Here we report our initial results in the form of an examination of the series $[Fe_4S_4(SC_6H_4\text{-}o\text{-}X)_4]^{2-}$, with X = OH, OMe, NH_2, and SMe. As will be demonstrated the X = OH species contains one five-coordinate Fe site in a cluster, certain properties of which depart from those of the standard $[Fe_4S_4(SR)_4]^{2-}$ (**1**) type.

Experimental Section

Preparation of Compounds. All operations were carried out under a pure dinitrogen atmosphere; solvents were distilled and degassed before use. *o*-Aminobenzenethiol and *o*-methoxybenzenethiol were commercial samples (Aldrich) and were used without further purification. *o*-Hydroxybenzenethiol[25] (**caution**: vessicant) and *o*-methylthiobenzenethiol[26] were prepared by published methods. ^1H NMR data refer to CD_3CN solutions at ~298 K.

$(Et_4N)_2[Fe_4S_4(SC_6H_4\text{-}o\text{-}X)_4]$ (X = OH, NH_2, OMe). These compounds were prepared by thiolate ligand substitution reactions.[8b] A typical preparation is described. A stirred slurry of 2.00 g (2.06 mmol) of $(Et_4N)_2[Fe_4S_4(S\text{-}t\text{-}Bu)_4]$[24] in 75 mL of acetonitrile was treated with 1.04 g (8.26 mmol) of $o\text{-}HOC_6H_4SH$ in 25 mL of acetonitrile. The solid dissolved and a red-brown color developed. Some solvent (~20 mL) was removed in vacuo and the solution was stirred for 4 h. The volume was reduced to ~50 mL and the solution was maintained at -20 °C. The solid was collected by filtration, washed with 25 mL of methanol, and dried in vacuo. Triplicate preparations afforded the product as red-black crystals in 85–93% yield. Analytical samples of this and other compounds were obtained by recrystallization from acetonitrile. Anal. Calcd for $C_{40}H_{60}Fe_4N_2O_4S_8$: C, 43.17; H, 5.43; Fe, 20.07; N, 2.52; S, 23.05. Found: C, 43.09; H, 5.35; Fe, 19.80; N, 2.60; S, 22.92. ^1H NMR: -5.75 (*p*-H), -6.06 (OH), -6.36 (*o*-H); -7.76 (d), -7.96 (*m*-H) ppm. The X = NH_2 and OMe cluster salts were isolated as red-black crystals in 80–90% yield. Anal. Calcd for $C_{40}H_{64}Fe_4N_6S_8$ (X = NH_2): C, 43.33; H, 5.82; Fe, 20.15; N, 7.58; S, 23.13. Found: C, 43.18; H, 5.75; Fe, 19.94; N, 7.42; S, 22.91. ^1H NMR: -4.60 (NH_2), -5.52 (*p*-H), -6.12 (*o*-H); -7.64, -7.76 (d) (*m*-H) ppm. Anal. Calcd for $C_{44}H_{68}Fe_4N_2O_2S_8$ (X = OMe): C, 45.21; H, 5.86; Fe, 19.11; N, 2.40; S, 21.94. Found: C, 44.93; H, 5.74; Fe, 19.00; N, 2.43; S, 21.86. ^1H NMR: -4.39 (OMe),

---

(4) Berg, J. M.; Holm, R. H. In "Metal Ions in Biology"; Spiro, T. G., Ed.; Wiley-Interscience: New York, 1982; Vol. 4, Chapter 1.

(5) Papaefthymiou, G. C.; Laskowski, E. J.; Frota-Pessôa, S.; Frankel, R. B.; Holm, R. H. *Inorg. Chem.* **1982**, *21*, 1723.

(6) Stephan, D. W.; Papaefthymiou, G. C.; Frankel, R. B.; Holm, R. H. *Inorg. Chem.* **1983**, *22*, 1550.

(7) Mascharak, P. K.; Hagen, K. S.; Spence, J. T.; Holm, R. H. *Inorg. Chim. Acta*, **1983**, *80*, 157.

(8) (a) $[Fe_4S_4(SCH_2Ph)_4]^{2-}$: Averill, B. A.; Herskovitz, T.; Holm, R. H.; Ibers, J. A. *J. Am. Chem. Soc.* **1973**, *95*, 3523. (b) $[Fe_4S_4(SPh)_4]^{2-}$: Que, L., Jr.; Bobrik, M. A.; Ibers, J. A.; Holm, R. H. *Ibid.* **1974**, *96*, 4168. (c) $[Fe_4S_4(SCH_2CH_2CO_2)_4]^{6-}$: Carrell, H. L.; Glusker, J. P.; Job, R.; Bruice, T. C. *Ibid.* **1977**, *99*, 3683. (d) $[Fe_4S_4(SCH_2CH_2OH)_4]^{2-}$: Christou, G.; Garner, C. D.; Drew, M. G. B.; Cammack, R. *J. Chem. Soc., Dalton Trans.* **1981**, 1550. (e) $[Fe_4S_4(S\text{-}t\text{-}Bu)_4]^{2-}$ (two crystalline forms): ref 7.

(9) Ghosh, D.; O'Donnell, S.; Furey, W., Jr.; Robbins, A. H.; Stout, C. D. *J. Mol. Biol.* **1982**, *158*, 73.

(10) For a review of ferredoxin site structures cf.: Stout, C. D. In "Metal Ions in Biology"; Spiro, T. G., Ed.; Wiley-Interscience: New York, 1982; Vol. 4, Chapter 3.

(11) Sweeney, W. V.; Rabinowitz, J. C. *Annu. Rev. Biochem.* **1980**, *49*, 139.

(12) This statement excludes structural[4] and electronic[6,13] differences among the reduced clusters **2** in the *solid* state. In solution these differences are much smaller, and current evidence favors the existence of an essentially constant tetragonally elongated $[Fe_4S_4]^{1+}$ core structure.[6,13] The detailed structure of an isoelectronic protein site is unknown.

(13) Laskowski, E. J.; Reynolds, J. G.; Frankel, R. B.; Foner, S.; Papaefthymiou, G. C.; Holm, R. H. *J. Am. Chem. Soc.* **1979**, *101*, 6562.

(14) Münck, E. *Adv. Chem. Ser.* **1981**, *No. 194*, 305.

(15) Averill, B. A. *Struct. Bonding (Berlin)* **1983**, *53*, 59.

(16) Kurtz, D. M., Jr.; McMillan, R. S.; Burgess, B. K.; Mortenson, L. E.; Holm, R. H. *Proc. Natl. Acad. Sci. U.S.A.* **1979**, *76*, 4986.

(17) (a) Münck, E.; Rhodes, H.; Orme-Johnson, W. H.; Davis, L. C.; Brill, W. J.; Shah, V. K. *Biochim. Biophys. Acta* **1975**, *400*, 32. (b) Zimmermann, R.; Münck, E.; Brill, W. J.; Shah, V. K.; Henzl, M. T.; Rawlings, J.; Orme-Johnson, W. H. *Ibid.* **1978**, *537*, 185. (c) Huynh, B. H.; Henzl, M. T.; Christner, J. A.; Zimmermann, R.; Orme-Johnson, W. H.; Münck, E. *Ibid.* **1980**, *623*, 124.

(18) Smith, B. E.; O'Donnell, M. J.; Lang, G.; Spartalian, K. *Biochem. J.* **1980**, *191*, 449.

(19) (a) Johnson, M. K.; Thomson, A. J.; Robinson, A. E.; Smith, B. E. *Biochim. Biophys. Acta* **1981**, *671*, 61. (b) Stephens, P. J.; McKenna, C. E.; Smith, B. E.; Nguyen, H. T.; McKenna, M.-C.; Thomson, A. J.; Devlin, F.; Jones, J. B. *Proc. Natl. Acad. Sci. U.S.A.* **1979**, *76*, 2585.

(20) Christou, G.; Mascharak, P. K.; Armstrong, W. H.; Papaefthymiou, G. C.; Frankel, R. B.; Holm, R. H. *J. Am. Chem. Soc.* **1982**, *104*, 2820.

(21) (a) Cleland, W. E.; Averill, B. A. *Inorg. Chim. Acta* **1981**, *56*, L9. (b) Cleland, W. E.; Holtman, D. A.; Sabat, M.; Ibers, J. A.; DeFotis, G. C.; Averill, B. A. *J. Am. Chem. Soc.* **1983**, *105*, 6021.

(22) Kanatzidis, M. G.; Ryan, M.; Coucouvanis, D.; Simopoulos, A.; Kostikas, A. *Inorg. Chem.* **1983**, *22*, 179. Et_2dtc = *N,N'*-diethyldithiocarbamate.

(23) (a) Bobrik, M. A.; Hodgson, K. O.; Holm, R. H. *Inorg. Chem.* **1977**, *16*, 1851. (b) Wong, G. B.; Bobrik, M. A.; Holm, R. H. *Ibid.* **1978**, *17*, 578.

(24) Johnson, R. W.; Holm, R. H. *J. Am. Chem. Soc.* **1978**, *100*, 5338.

(25) Greenwood, D.; Stevenson, H. A. *J. Chem. Soc.* **1953**, 1514. Cabiddu, S.; Maccioni, A.; Secci, M.; Solinas, V. *Gazz. Chim. Ital.* **1969**, *99*, 397.

(26) Livingstone, S. E. *J. Chem. Soc.* **1956**, 437.

Table I. Summary of Crystal Data, Intensity Collection, and Structure Refinement for $(Et_4N)_2[Fe_4S_4(SC_6H_4\text{-}o\text{-}OH)_4]$

quantity	data
formula (M_r)	$C_{40}H_{60}Fe_4N_2O_4S_8$ (1112.83)
a, Å	11.786 (3)
b, Å	20.701 (6)
c, Å	20.536 (7)
β, deg	94.42 (2)
cryst system	monoclinic
Z	4
V, Å^3	4996
d_{calcd}, g/cm^3	1.479
d_{obsd}, g/cm^3	1.47[a]
space group	$P2_1/c$ (C_{2h}^5)
cryst dimens, mm	0.30 × 0.35 × 0.60
radiation	Mo Kα (λ = 0.71069 Å)
abs coeff, μ, cm^{-1}	15.2
transmission factors	0.455 to 0.359
takeoff angle, deg	3.0
scan speed, deg/min	3.0–30.0 ($\theta/2\theta$ scan)
scan range, deg	1.0 below Kα_1 to 1.0 above Kα_2
bkgd: scan time	0.25
data collected	7026
no. of unique data ($F_o^2 > 2.5\sigma(F_o^2)$)	4993
no. of variables	523
R, %	5.6
R_w, %	4.7

[a] Determined by flotation in n-hexane/CCl_4.

−5.30 (p-H), −5.97 (o-H); −7.77 (d), −8.19 (m-H) ppm.

$(n\text{-}Bu_4N)_2[Fe_4S_4(SC_6H_4\text{-}o\text{-}SMe)_4]$. This compound was prepared by the preceding method with use of $(n\text{-}Bu_4N)_2[Fe_4S_4(S\text{-}t\text{-}Bu)_4]$,[8a] isolated in 90% yield as red-brown flaky crystals, and recrystallized from acetonitrile. Anal. Calcd for $C_{60}H_{100}Fe_4N_2S_{12}$: C, 49.44; H, 6.92; Fe, 15.33; N, 1.92; S, 26.40. Found: C, 49.48; H, 7.02; Fe, 15.25; N, 2.04; S, 26.29. Other salts of this cluster were not obtained in analytical purity. ^{1}H NMR: −3.51 (SMe), −5.42 (p-H), −6.03 (o-H); −8.12 (d), −8.19 (m-H) ppm.

Salts of $[Fe_4S_4(SC_6H_4\text{-}p\text{-}X)_4]^{2-}$. The following compounds were prepared by the ligand substitution method using commercially available thiols and were purified by recrystallization from acetonitrile: $(n\text{-}Bu_4N)_2[Fe_4S_4(SC_6H_4\text{-}p\text{-}OH)_4]$: −5.69 ($o$-H), −6.59 (OH), −7.62 ($m$-H) ppm; $(n\text{-}Bu_4N)_2[Fe_4S_4(SC_6H_4\text{-}p\text{-}OMe)_4]$: −3.88 (OMe), −5.82 ($o$-H), −7.72 ($m$-H) ppm; $(Et_4N)_2[Fe_4S_4(SC_6H_4\text{-}p\text{-}NH_2)_4]$: −4.21 ($NH_2$), −5.66 ($o$-H), −7.47 ($m$-H) ppm. These compounds were not analyzed but, as for meta-substituted clusters, their ^{1}H NMR spectra[27] and electrochemical properties[7,28,29] (vide infra) are entirely characteristic of the cluster formulation **1**. Clusters with X = OH[30] and OMe[31] have been previously isolated as other salts.

X-ray Data Collection and Reduction. Red-black air-sensitive crystals, grown by slow cooling of an acetonitrile solution of $(Et_4N)_2[Fe_4S_4(SC_6H_4\text{-}o\text{-}OH)_4]$, were sealed in glass capillaries under argon. The unit cell dimensions and orientation matrices were calculated from 25 reflections (25° ≤ 2θ ≤ 30°). Diffraction experiments were performed at ambient temperature on a Nicolet R3m four-circle automated diffractometer with a Mo X-ray source equipped with a graphite monochromator. The crystal and machine parameters used in the data collection are summarized in Table I. Three check reflections were measured every 123 reflections; these exhibited no significant decay over the duration of data collection. The data were processed with the program XTAPE of the SHELXTL package (Nicolet XRD Corp., Fremont, CA). Empirical absorption corrections were applied with the program XEMP. The compound crystallizes in the monoclinic space group $P2_1/c$, uniquely determined by the systematic absences $h0l$ ($h = 2n + 1$) and $0k0$ ($k = 2n + 1$).

Structure Solution and Refinement. All calculations were carried out with the SHELXTL programs. Atomic scattering factors were taken from the tabulation of Cromer and Waber.[32] The direct-methods program MULTAN revealed the atomic positions of the Fe_4S_4 cluster core. All remaining non-hydrogen atoms were located, and their positional parameters were refined by using difference Fourier maps and blocked cascade least-squares refinement. Isotropic refinement of all non-hydrogen atoms converged at R = 11.0%. All non-hydrogen atoms were subsequently refined by using an anisotropic thermal model. In the last stage of refinement, fixed contributions from hydrogen atoms with thermal parameters set at 1.2× that of the bonded carbon atoms were included. The hydrogens of the hydroxyl groups could not be adequately discerned in a final difference Fourier map, and they were not included in the structural model. Final R factors and other data are included in Table I. Positional parameters of the anion are listed in Table II, and selected interatomic distances and angles are collected in Table III.[33]

Table II. Atom Coordinates (×10^4) for $[Fe_4S_4(SC_6H_4\text{-}o\text{-}OH)_4]^{2-}$

atom	x	y	z
Fe(1)	2630 (1)[a]	508 (1)	2910 (1)
Fe(2)	972 (1)	1303 (1)	2229 (1)
Fe(3)	817 (1)	1017 (1)	3508 (1)
Fe(4)	2418 (1)	1864 (1)	3161 (1)
S(1)	736 (1)	292 (1)	2661 (1)
S(2)	2857 (1)	1419 (1)	2200 (1)
S(3)	2643 (1)	1054 (1)	3908 (1)
S(4)	513 (1)	2018 (1)	3032 (1)
S(5)	3997 (1)	−92 (1)	2430 (1)
S(6)	−43 (2)	1416 (1)	1242 (1)
S(7)	−217 (1)	731 (1)	4353 (1)
S(8)	3616 (2)	2707 (1)	3394 (1)
O(1)[b]	2825 (4)	−387 (2)	3587 (2)
C(11)	4051 (5)	−826 (3)	2857 (3)
C(12)	3456 (5)	−900 (3)	3416 (3)
C(13)	3493 (6)	−1463 (3)	3765 (3)
C(14)	4119 (6)	−1988 (3)	3572 (4)
C(15)	4722 (6)	−1928 (4)	3024 (4)
C(16)	4696 (5)	−1353 (3)	2675 (3)
O(2)	−969 (7)	131 (4)	1028 (4)
C(21)	−1439 (6)	1159 (3)	1396 (3)
C(22)	−1756 (7)	524 (4)	1238 (4)
C(23)	−2862 (7)	316 (4)	1297 (4)
C(24)	−3644 (7)	724 (4)	1518 (4)
C(25)	−3329 (7)	1329 (4)	1681 (4)
C(26)	−2229 (7)	1575 (4)	1631 (4)
O(3)	−1886 (4)	466 (3)	5278 (2)
C(31)	−1696 (5)	794 (3)	4169 (3)
C(32)	−2377 (5)	662 (3)	4675 (3)
C(33)	−3541 (6)	711 (4)	4584 (4)
C(34)	−4058 (7)	868 (5)	3991 (5)
C(35)	−3399 (7)	988 (5)	3478 (4)
C(36)	−2219 (6)	956 (4)	3570 (4)
O(4)	4705 (5)	2369 (3)	4700 (3)
C(41)	3262 (6)	3029 (3)	4147 (3)
C(42)	3902 (6)	2848 (4)	4723 (4)
C(43)	3717 (7)	3162 (4)	5308 (4)
C(44)	2908 (8)	3630 (4)	5326 (4)
C(45)	2247 (9)	3791 (4)	4779 (5)
C(46)	2434 (7)	3495 (4)	4183 (4)

[a] Estimated standard deviations in the least significant figure(s) are given in this and subsequent tables. [b] For ring atom numbering scheme cf. Figure 1.

Other Physical Measurements. All measurements were made under anaerobic conditions. Absorption spectra were recorded on a Cary Model 219 spectrophotometer. Magnetic susceptibilities were determined in the solid state by the Faraday method ($HgCo(NCS)_4$ calibrant). ^{1}H NMR spectra and solution susceptibilities were measured with a Bruker WM-300 spectrometer. Chemical shifts at fields below that of the Me_4Si internal reference are designated as negative. Cyclic voltammetry (CV) and differential pulse polarography (DPP) of DMF solutions were performed with standard PAR instrumentation. DPP measurements utilized a 25-mV modulation amplitude and a scan rate of 5 mV/s. The working electrode was glassy carbon and the reference electrode was a saturated calomel electrode (SCE); all solutions contained 0.1 M $(n\text{-}Bu_4N)ClO_4$ as the supporting electrolyte. Mössbauer spectra were measured with a conventional constant acceleration spectrometer having a ^{57}Co source in

---

(27) Reynolds, J. G.; Laskowski, E. J.; Holm, R. H. *J. Am. Chem. Soc.* **1978**, *100*, 5315.

(28) DePamphilis, B. V.; Averill, B. A.; Herskovitz, T.; Que, L., Jr.; Holm, R. H. *J. Am. Chem. Soc.* **1974**, *96*, 4159.

(29) Cambray, J.; Lane, R. W.; Wedd, A. G.; Johnson, R. W.; Holm, R. H. *Inorg. Chem.* **1977**, *16*, 2565.

(30) Rzaigui, M.; Panossian, R.; Benlian, D. *Rev. Chim. Miner.* **1980**, *17*, 586.

(31) Hill, C. L.; Steenkamp, D. J.; Holm, R. H.; Singer, T. P. *Proc. Natl. Acad. Sci. U.S.A.* **1977**, *74*, 547.

(32) Cromer, D. T.; Waber, J. T. "International Tables for X-Ray Crystallography"; Kynoch Press: Birmingham, England; 1974.

(33) See paragraph at the end of this article regarding supplementary material.

Table III. Selected Interatomic Distances (Å) and Angles (deg) for $[Fe_4S_4^*(SC_6H_4\text{-}o\text{-}OH)_4]^{2-}$

Fe–O[b]		Fe–S	
Fe(1)–O(1)	2.318 (5)[a]	Fe(1)–S(5)	2.313 (3)
		Fe–S	
Fe(2)–S(6)	2.286 (3)	Fe(4)–S(8)	2.273 (3)
Fe(3)–S(7)	2.274 (2)	mean (of 3)	2.278 (7)
		Fe–S*	
Fe(1)–S(1)	2.296 (2)	Fe(3)–S(1)	2.294 (2)
Fe(1)–S(2)	2.411 (3)	Fe(3)–S(3)	2.244 (2)
Fe(1)–S(3)	2.339 (2)	Fe(3)–S(4)	2.308 (3)
Fe(2)–S(1)	2.298 (3)	Fe(4)–S(2)	2.273 (2)
Fe(2)–S(2)	2.241 (2)	Fe(4)–S(3)	2.274 (2)
Fe(2)–S(4)	2.310 (3)	Fe(4)–S(4)	2.263 (2)
		mean	2.30 (5)
		Fe···Fe	
Fe(1)···Fe(2)	2.839 (2)	Fe(2)···Fe(3)	2.711 (2)
Fe(1)···Fe(3)	2.755 (2)	Fe(2)···Fe(4)	2.722 (2)
Fc(1)···Fe(4)	2.868 (2)	Fe(3)···Fe(4)	2.710 (2)
		mean	2.77 (7)
		C–O	
C(12)–O(1)	1.359 (8)	C(32)–O(3)	1.386 (8)
C(22)–O(2)	1.330 (11)	C(42)–O(4)	1.374 (10)
		mean	1.36 (2)
		C–S	
C(11)–S(5)	1.753 (7)	C(31)–S(7)	1.760 (6)
C(21)–S(6)	1.780 (7)	C(41)–S(8)	1.763 (7)
		mean	1.76 (1)
		C–C	
C(11)–C(12)	1.399 (9)	C(14)–C(15)	1.383 (11)
C(12)–C(13)	1.368 (9)	C(15)–C(16)	1.387 (10)
C(13)–C(14)	1.388 (10)	C(16)–C(11)	1.397 (9)
		mean	1.39 (1)
other rings: range 1.34 (1)–1.40 (1), mean 1.38 (2)			
		O···S	
O(1)···S(5)	2.904 (4)	O(2)···S(1)	3.79
O(2)···S(6)	2.897 (5)	O(2)···S(2)	5.62
O(3)···S(7)	2.891 (5)	O(3)···S(1)	6.41
O(4)···S(8)	2.966 (5)	O(3)···S(3)	6.34
		O(4)···S(2)	5.77
		O(4)···S(3)	3.92

		Fe–Fe–Fe	
Fe(2)–Fe(1)–Fe(3)	57.9 (1)	Fe(1)–Fe(3)–Fe(2)	62.6 (1)
Fe(3)–Fe(1)–Fe(4)	57.6 (1)	Fe(1)–Fe(3)–Fe(4)	63.3 (1)
Fe(2)–Fe(1)–Fe(4)	57.0 (1)	Fe(2)–Fe(3)–Fe(4)	60.3 (1)
Fe(1)–Fe(2)–Fe(3)	59.5 (1)	Fe(1)–Fc(4)–Fe(2)	61.0 (1)
Fe(3)–Fe(2)–Fe(4)	59.8 (1)	Fe(1)–Fe(4)–Fe(3)	59.1 (1)
Fe(1)–Fe(2)–Fe(4)	62.0 (1)	Fe(2)–Fe(4)–Fe(3)	59.9 (1)
		mean	60.0
		Fe–S*–Fe	
Fe(1)–S(1)–Fe(2)	76.3 (1)	Fe(1)–S(3)–Fe(3)	73.9 (1)
Fe(1)–S(1)–Fe(3)	73.8 (1)	Fe(1)–S(3)–Fe(4)	76.9 (1)
Fe(2)–S(1)–Fe(3)	72.4 (1)	Fe(3)–S(3)–Fe(4)	73.7 (1)
Fe(1)–S(2)–Fe(2)	75.1 (1)	Fe(2)–S(4)–Fe(3)	71.9 (1)
Fe(1)–S(2)–Fe(4)	75.4 (1)	Fe(2)–S(4)–Fe(4)	73.0 (1)
Fe(2)–S(2)–Fe(4)	74.2 (1)	Fe(3)–S(4)–Fe(4)	72.7 (1)
		mean	74.1
		S*–Fe–S*	
S(1)–Fe(1)–S(2)	99.7 (1)	S(1)–Fe(3)–S(3)	106.4 (1)
S(1)–Fe(1)–S(3)	103.3 (1)	S(1)–Fe(3)–S(4)	105.7 (1)
S(2)–Fe(1)–S(3)	99.1 (1)	S(3)–Fe(3)–S(4)	103.8 (1)
S(1)–Fe(2)–S(2)	104.9 (1)	S(2)–Fe(4)–S(3)	105.3 (1)
S(1)–Fe(2)–S(4)	105.5 (1)	S(2)–Fe(4)–S(4)	104.2 (1)
S(2)–Fe(2)–S(4)	103.8 (1)	S(3)–Fe(4)–S(4)	104.3 (1)
		mean	103.8
		S*–Fe–S	
S(2)–Fe(1)–S(5)	92.8 (1)	range (of 9)	106.5 (1)–118.8 (1)
S(1)–Fe(1)–S(5)	119.9 (1)		
S(3)–Fe(1)–S(5)	132.4 (1)		
O–Fe–S*		O–Fe–S	
O(1)–Fe(1)–S(1)	91.6 (1)	O(1)–Fe(1)–S(5)	77.7 (1)
O(1)–Fe(1)–S(3)	82.3 (1)		
O(1)–Fe(1)–S(2)	167.9 (1)		

	volumes, Å^3	
	this cluster	$[Fe_4S_4(SPh)_4]^{2-}$[c]
Fe_4	2.49	2.41
S_4	5.55	5.54
Fe_4S_4	9.77	9.55

[a] The standard deviation of the mean was estimated from $\sigma \approx s = [(\Sigma x_i^2 - n\bar{x}^2)/(n-1)]^{1/2}$. [b] Nonbonded distances: Fe(2)–O(2), 5.57; Fe(3)–O(3), 5.14; Fe(4)–O(4), 4.13 Å. [c] Reference 4.

a Rh matrix maintained at room temperature. Isomer shifts are referenced to Fe metal at 4.2 K.

Results and Discussion

Synthesis of Clusters. Four examples of the cluster type $[Fe_4S_4(SC_6H_4\text{-}o\text{-}X)_4]^{2-}$ were synthesized by means of the ligand substitution reaction 1[4,8b] and were isolated in good yields as Et_4N^+

$$[Fe_4S_4(S\text{-}t\text{-}Bu)_4]^{2-} + 4XC_6H_4\text{-}o\text{-}SH \xrightarrow{MeCN} \underset{\textbf{3–6}}{[Fe_4S_4(SC_6H_4\text{-}o\text{-}X)_4]^{2-}} + 4t\text{-}BuSH \quad (1)$$

3, X = OH; **4**, X = NH_2; **5**, X = OMe; **6**, X = SMe

(**3–5**) or n-Bu_4N^+ (**6**) salts. A set of para-substituted clusters $[Fe_4S_4(SC_6H_4\text{-}p\text{-}X)_4]^{2-}$ (X = OH, NH_2, OMe), required for comparison of certain properties, was also prepared by this procedure. The rigid ortho-substituted benzenethiolate ligands were utilized with the intention of promoting intracluster closure of five-membered chelate rings. Of the more than 50 clusters containing the $[Fe_4S_4]^{2+}$ core that have been prepared,[4] only a few contain potentially chelating RS ligands (R = $(CH_2)_{2,3}CO_2^-$,[8c,34–36] CH_2CH_2OH,[8d,37] CMe_2CH_2OH,[7] CMe_2CH_2NHPh[7]). There is no clear evidence that in solution these clusters contain chelate rings, and X-ray structural results

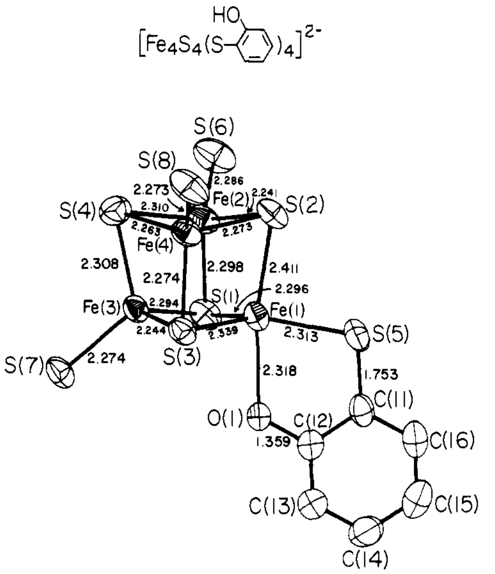

Figure 1. Structure of $[Fe_4S_4(SC_6H_4\text{-}o\text{-}OH)_4]^{2-}$ showing atom numbering scheme, 50% probability ellipsoids, and selected bond distances; the three o-C_6H_4OH substituted ligands with uncoordinated hydroxyl groups are omitted.

---

(34) Job, R. C.; Bruice, T. C. *Proc. Natl. Acad. Sci. U.S.A.* **1975**, *72*, 2478.

(35) Maskiewicz, R.; Bruice, T. C. *J. Chem. Soc., Chem. Commun.* **1978**, 703.

(36) Henderson, R. A.; Sykes, A. G. *Inorg. Chem.* **1980**, *19*, 3103.

(37) Hill, C. L.; Renaud, J.; Holm, R. H.; Mortenson, L. E. *J. Am. Chem. Soc.* **1977**, *99*, 2549.

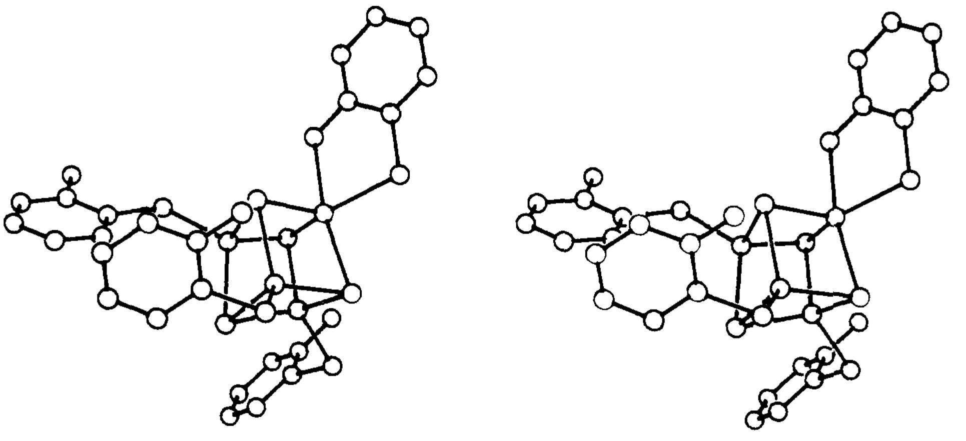

Figure 2. Stereoview of the structure of $[Fe_4S_4(SC_6H_4\text{-}o\text{-}OH)_4]^{2-}$.

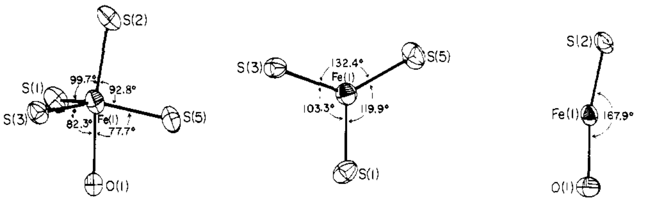

Figure 3. Structural features of the Fe(1)S_4O portion of $[Fe_4S_4(SC_6H_4\text{-}o\text{-}OH)_4]^{2-}$ showing bond angles.

in two cases, $[Fe_4S_4(SCH_2CH_2CO_2)_4]^{6-}$[8c] and $[Fe_4S_4(SCH_2CH_2OH)_4]^{2-}$,[8d] reveal the absence of such rings in the solid state. As will be shown, cluster **3** possesses one chelate ring as its crystalline Et_4N^+ salt. Single crystals of diffraction quality have not yet been obtained for salts of clusters **4**-**6**.

Structure of $[Fe_4S_4(SC_6H_4\text{-}o\text{-}OH)_4]^{2-}$. The crystal structure of the Et_4N^+ salt consists of well-separated cations and anions. Cation structures are unexceptional.[33] The structure of the anion is presented in Figure 1; a stereoview of the entire cluster is provided in Figure 2. It is immediately evident that the cluster contains *one* chelate ring. The environment of the chelated, five-coordinate atom Fe(1) is depicted in more detail in Figure 3. Hydroxyl hydrogen atoms were not located in the structure refinement. However, elemental analysis and the existence of two cations in the crystal structure require the presence of terminal ligands as monoanions. With reference to Figures 1-3, Table III, and previous structural summaries and analysis of $[Fe_4S_4]^{2+}$ clusters,[4,7] the remaining principal structural features of $[Fe_4S_4(SC_6H_4\text{-}o\text{-}OH)_4]^{2-}$ are summarized.

(a) The $[Fe_4S_4]^{2+}$ Core. (i) The core departs from the compressed tetragonal stereochemistry (four short and eight long Fe-S bonds approximately parallel and perpendicular, respectively, to an idealized or imposed $\bar{4}$ axis) found for all clusters having the same core oxidation level and four identical monodentate ligands.[38] Owing, in particular, to an irregular arrangement of Fe-S bond lengths the core structure does not achieve mirror symmetry. (ii) Each Fe_2S_2 face of the core is a nonplanar rhomb, with the smallest (±0.12 Å) and largest (±0.17 Å) atom displacements from weighted least-squares planes found with the Fe(1,3)S(1,3) and Fe(3,4)S(3,4) planes, respectively. Diagonal core planes are nearly perfect. (iii) All core Fe-S and Fe··Fe distances fall within the ranges of 2.23-2.33 and 2.72-2.79 Å, respectively, found for other isoelectronic cores except for three distances involving chelated Fe(1). These are Fe(1)-S(2) = 2.411 (3) Å, Fe(1)···Fe(2) = 2.839 (2) Å, and Fe(1)···Fe(4) = 2.868 (2) Å, which fall decisively ($\gg 3\sigma$) outside these ranges. The first of the distances may be lengthened by virtue of a weak trans effect of coordinated O(1). (iv) Volumes of the imperfect tetrahedral Fe_4 and S_4 portions (Table III) are equal to the upper limits known for this type of cluster. The Fe_4S_4 volume is 2.25% larger than that of $[Fe_4S_4(SPh)_4]^{2-}$ and is the largest $[Fe_4S_4]^{2+}$ core known.[4,7] This relative volume enlargement is primarily a consequence of the longer Fe(1) bond distances in (iii).

(b) Terminal Ligation. (v) The 4.13-5.57-Å range of Fe··O distances involving oxygen atoms of the substituents of S(6-8) demonstrates the lack of interaction of these atoms with any Fe atom. (vi) Terminal Fe-S distances to the three monodentate ligands are biased to the high side of the range (2.23-2.27 Å) for other clusters; however, the mean distance of 2.278 (7) Å is not distinguishable from that for $[Fe_4S_4(SPh)_4]^{2-}$ (2.263 (7) Å[8b]). (vii) The Fe(1)-S(5) distance of 2.313 (3) Å is only 0.035 Å longer than the mean of the other terminal Fe-S distances, a difference presumably due to the fact that Fe(1) is five-coordinate. The Fe(1)-O(1) separation of 2.318 (5) Å is some 0.45 Å *longer* than the mean value (1.865 (17) Å) of Fe-O bond lengths in $[Fe_4S_4(OPh)_4]^{2-}$.[21b] These chelate ring bond distances establish the presence of a coordinated -OH rather than a -SH group and afford the description of the Fe(1)-O(1) bond as a weak, i.e., *secondary*, interaction.[39] (viii) The Fe(1)S(1-3,5)O(1) coordination unit (Figure 3) is better described as a distorted trigonal bipyramid (TBP), with a S(1,3,5) equatorial plane and O(1) + S(1) axial ligands, than as a distorted square bipyramid (SP). The axial bond angle is 167.9 (1)°, two of the three equatorial bond angles are ≥120°, and five of the six axial/equatorial bond angles fall in the 92-100° interval. Dihedral angles with these ranges and mean values enclose the indicated TBP edges: three equatorial, 32.2-70.1°, 51.9°; six axial, 95.0-116.2°, 104.3°. Angular shape characteristics for a perfect TBP with all bond lengths equal are 53.1° for equatorial and 101.5° for axial edges.[41] Among numerous five-coordinate structures these bond and dihedral angles are close to those of $[Co(pyO)_5](ClO_4)_2$,[41,42] for which a distorted TBP description is preferred for the cation.[42]

Two other cubane-like Fe_4S_4 clusters containing five-coordinate Fe atoms, in distorted SP arrangements, have been reported. The structure of $[Fe_4S_4(S_2C_2(CF_3)_2)_4]^{2-}$,[43] originally prepared by Balch,[44] contains four such Fe sites. Because of the dithiolene nature of the chelating ligands the core oxidation level is uncertain. However, from structural and other evidence, pursued at length elsewhere,[43,45] it is certain that this cluster does not contain a core

---

[38] A different type of distortion from core cubic symmetry has been found for certain $[Fe_4S_4X_2Y_2]^{2-}$ clusters in which X and Y are different monodentate ligands: Coucouvanis, D.; private communication.

[39] Prior investigations of complexes of *o*-HSC_6H_4OH have dealt with bis(chelate) species not containing Fe.[40] The lack of structural data for these complexes precludes comparison of chelate ring dimensions with those of cluster **3**.

[40] Balch, A. L.; Röhrscheid, F.; Holm, R. H. *J. Am. Chem. Soc.* **1965**, *87*, 2301. Balch, A. L. *Ibid.* **1969**, *91*, 1948.

[41] Muetterties, E. L.; Guggenberger, L. J. *J. Am. Chem. Soc.* **1974**, *96*, 1748.

[42] Coyle, B. A.; Ibers, J. A. *Inorg. Chem.* **1970**, *9*, 767. pyO = pyridine *N*-oxide.

[43] Lemmen, T. H.; Kocal, J. A.; Ko, F. Y.-K.; Chen, M. W.; Dahl, L. F. *J. Am. Chem. Soc.* **1981**, *103*, 1932.

[44] Balch, A. L. *J. Am. Chem. Soc.* **1969**, *91*, 6962.

[45] Chu, C. T.-W.; Lo, F. Y.-K.; Dahl, L. F. *J. Am. Chem. Soc.* **1982**, *104*, 3409.

Table IV. Mössbauer Spectral and Magnetic Properties of $[Fe_4S_4(SC_6H_4\text{-}o\text{-}X)_4]^{2-}$ and Related Clusters

cluster	T, K	δ,[a] mm/s	ΔE_Q, mm/s	Γ, mm/s	% A[b]	μ, μ_B (~298 K)
$[Fe_4S_4(SPh)_4]^{2-}$ [c]	4.2	0.35	1.10	-	100	2.17
$[Fe_4S_4(SC_6H_4\text{-}o\text{-}NH_2)_4]^{2-}$ [d]	4.2	0.33	0.88	0.34	100	2.25
$[Fe_4S_4(SC_6H_4\text{-}o\text{-}SMe)_4]^{2-}$ [d]	4.2	0.32 (A)	0.85	0.38	57	2.20
		0.54 (B)	1.87	0.38	43	
	80	0.31 (A)	0.82	0.38	57	
		0.53 (B)	1.86	0.40	43	
$[Fe_4S_4(SC_6H_4\text{-}o\text{-}OH)_4]^{2-}$ [d]	4.2	0.31 (A)	0.75	0.26	21	2.11
		0.36 (B)	1.22	0.34	56	
		0.51 (C)	1.84	0.28	23	
	80	0.30 (A)	0.76	0.26	22	
		0.34 (B)	1.23	0.34	55	
		0.49 (C)	1.82	0.26	23	
MeCN soln	4.2	0.34 (A)	1.13	0.39	93[e]	2.15 (249 K), 2.18 (256 K),
	80	0.32 (A)	1.03	0.43	97[f]	2.26 (297 K)
$[Fe_4S_4(SC_6H_4\text{-}o\text{-}OMe)_4]^{2-}$ [d]	4.2	0.36	1.06	0.36	49	2.21
		0.40	1.50	0.36	51	
$[Fe_4S_4(OPh)_4]^{2-}$ [g]	4.2	0.38[h]	1.21	0.32	-	2.44
$[Fe_4S_4(SPh)_2(Et_2dtc)_2]^{2-}$ [i]	77	0.27[h]	1.34	-	-	2.56 (Me_2SO soln)
		0.62[h]	1.67	-	-	
A. vinelandii FeMo protein[j] P clusters	4.2	0.52[h] (D)	0.81		~75	-
		0.57[h] (Fe^{2+})	3.02		~25	

[a] Relative to Fe metal at 4.2 K; to convert to values at 298 K vs. Fe metal add 0.12 mm/s. [b] Percent of total absorption. [c] References 5 and 46a. [d] Solid state. [e] Minority spectral component present with $\delta = 0.55$, $\Delta E_Q = 1.62$, $\Gamma = 0.40$ mm/s; $A = 7\%$. [f] Minority spectral component present with $\delta = 0.43$, $\Delta E_Q = 1.4$, $\Gamma = 0.43$ mm/s; $A = 3\%$. [g] Reference 21b. [h] Literature data corrected to Fe metal at 4.2 K. [i] Reference 22. [j] References 17a and 17c

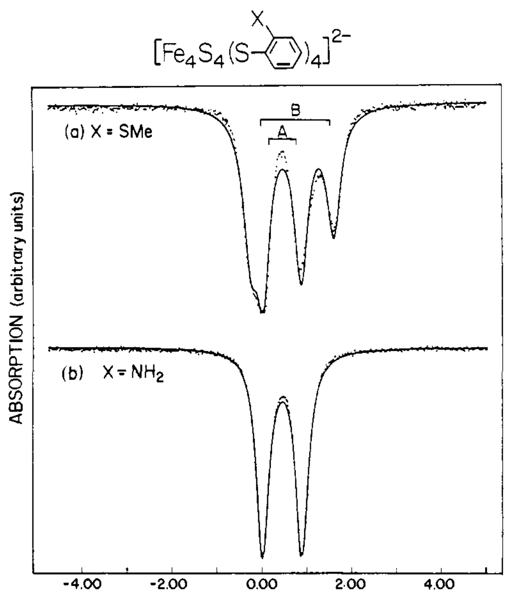

Figure 4. Mössbauer spectra (solid state, 4.2 K) of $[Fe_4S_4(SC_6H_4\text{-}o\text{-}X)_4]^{2-}$ clusters: (a) X = SMe (**6**); doublets A and B (Table IV) are indicated; (b) X = NH_2 (**4**). In this and the following figure the solid lines are least-squares fits of the data using the parameters in Table IV.

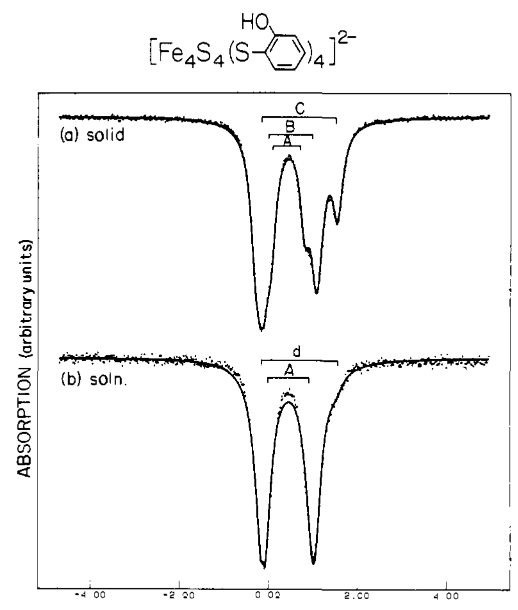

Figure 5. Mössbauer spectra (4.2 K) of $[Fe_4S_4(SC_6H_4\text{-}o\text{-}OH)_4]^{2-}$ in the solid state (a) and in acetonitrile solution (b). Doublets A–C (Table IV) in spectrum a are indicated; the doublet d in spectrum b is an unidentified minority component accounting for about ~7% of the total absorbance (footnote *e*, Table IV).

electronically equivalent to type **1** clusters. The cluster $[Fe_4S_4(SPh)_2(Et_2dtc)_2]^{2-}$ (**7**) has the $[Fe_4S_4]^{2+}$ core, two five-coordinate

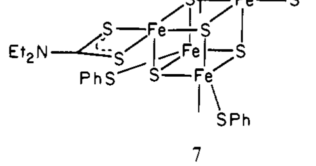

7

Fe sites, and imposed C_2 symmetry.[22] The chelate ligands are unsymmetrically bound, with Fe–S distances of 2.552 (4) and 2.436 (4) Å. A conspicuous effect of these ligands is to cause an asymmetry in and elongation of the dimensions of the Fe_2S_2 face containing both chelated Fe atoms. The two Fe–S distances are 2.309 (4) and 2.364 (4) Å and the Fe··Fe separation is 3.053 (3) Å. Other distances are within or very close to the ranges in (iii) and (vi) above.

Solid-State Properties of $[Fe_4S_4(SC_6H_4\text{-}o\text{-}X)_4]^{2-}$. Mössbauer spectra of clusters **3–6** are presented in Figures 4 and 5 with least-squares fits to the data based on the parameters in Table IV. In the solid state at 4.2–80 K the spectra are of two distinct types. The spectrum of $[Fe_4S_4(SC_6H_4\text{-}o\text{-}NH_2)_4]^{2-}$ (**4**, Figure 4b) has an isomer shift δ, quadrupole splitting ΔE_Q, and line width Γ entirely typical of $[Fe_4S_4(SR)_4]^{2-}$ clusters with R substituents lacking secondary interaction sites. Such clusters exhibit one or two closely overlapping quadrupole doublets with δ = 0.32–0.36

Table V. Solution Properties of $[Fe_4S_4(SC_6H_4\text{-}o,p\text{-}X)_4]^{2-}$ Clusters

cluster	E_p, V[a,b] 2−/3−	3−/4−[e]	λ_{max} (ϵ_M),[a] nm
$[Fe_4S_4(SC_6H_4\text{-}o\text{-}OH)_4]^{2-}$	−0.88	−1.51	293 (39 900), 371 (sh, 24 400), 440 (19 300)
$[Fe_4S_4(SC_6H_4\text{-}o\text{-}OMe)_4]^{2-}$	−1.15	−1.78	296 (47 900), 376 (sh, 22 700), 463 (18 200)
$[Fe_4S_4(SC_6H_4\text{-}o\text{-}NH_2)_4]^{2-}$	−1.07	−1.69	306 (37 700), 383 (sh, 22 000), 480 (17 900)
$[Fe_4S_4(SC_6H_4\text{-}o\text{-}SMe)_4]^{2-}$	−1.00	−1.70	311 (sh, 47 700), 380 (sh, 27 100), 476 (22 600)
$[Fe_4S_4(SC_6H_4\text{-}p\text{-}OH)_4]^{2-}$	−1.12	−1.86	304 (sh, 30 100), 345 (sh, 19 300), 477 (16 300)
$[Fe_4S_4(SC_6H_4\text{-}p\text{-}OMe)_4]^{2-}$	−1.09	−1.82	305 (sh, 28 300), 360 (sh, 17 900), 468 (15 400)
$[Fe_4S_4(SC_6H_4\text{-}p\text{-}NH_2)_4]^{2-}$	−1.20	−1.86	314 (sh, 34 600), 366 (sh, 21 100), 499 (18 800)
$[Fe_4S_4(SPh)_4]^{2-}$	−1.03[c]	−1.73[c]	260 (45 000), 350 (sh, 20 000), 457 (17 700)[d]

[a] DMF solution. [b] E_p from DPP, vs. SCE. [c] Reference 47. [d] Reference 28. [e] Irreversible reaction.

mm/s at 4.2–80 K.[6,46] It is concluded that the o-NH_2 groups do not appreciably interact with the core. The spectra of $[Fe_4S_4(SC_6H_4\text{-}o\text{-}SMe)_4]^{2-}$ (**6**, Figure 4a) and $[Fe_4S_4(SC_6H_4\text{-}o\text{-}OH)_4]^{2-}$ (**3**, Figure 5a) are more complicated. Cluster **3** shows three quadrupole doublets in the approximate intensity ratio A:B:C = 1:2:1. Assignments of the doublets cannot be proven; however, the following are reasonable. Because doublets A and B have the more usual δ and ΔE_Q values they are considered to be associated with Fe atoms in conventional tetrahedral sites. Atoms Fe(2,4) are assigned to B and atom Fe(3) to A. The former atoms are paired on the basis of mirror pseudosymmetry, structural feature iii. Doublet C, with the unusual δ = 0.49–0.51 mm/s and the largest quadrupole splitting at 4.2–80 K, is assigned to Fe(1), which is influenced by the secondary bonding interaction with O(1). The spectrum of cluster **6** was fit with two doublets of ~1:1 intensity ratio. Doublet A has unexceptional parameters but doublet B exhibits δ and ΔE_Q values very close to those of doublet C of **3**. These results are interpreted to mean that the polycrystalline sample of **6** has, on average, two tetrahedral Fe sites and two other Fe sites subject to secondary interactions with o-SMe groups. The spectrum of $[Fe_4S_4(SC_6H_4\text{-}o\text{-}OMe)_4]^{2-}$ (**5**, not shown) appears to reflect an intermediate situation in which the doublet with δ = 0.40 mm/s and ΔE_Q = 1.50 mm/s possibly indicates very weak secondary interactions involving ~50% of the Fe sites.

Magnetic moments per cluster for **3**–**6** in the solid state at ambient temperature (Table IV) are nearly constant and very close to those of type **1** clusters with no R-substituent coordinating groups.[5] The low values arise from antiferromagnetic spin coupling, which has been treated elsewhere.[5] Application of a 60-kOe external field results in a 60-kOe field at the nuclei and no hyperfine field, indicating the absence of paramagnetic components and retention by **3** of the spin-coupling interactions and attendant singlet ground state characteristic of type **1** clusters.

Solution Properties of $[Fe_4S_4(SC_6H_4\text{-}o\text{-}X)_4]^{2-}$. Certain properties were examined in solution for the purpose of characterization, especially with regard to the presence or absence of secondary interactions in the ortho-substituted clusters. Absorption spectral and electrochemical data, including for comparison purposes results for para-substituted clusters and $[Fe_4S_4(SPh)_4]^{2-}$,[28,47] are collected in Table V. Absorption spectra of clusters **3**–**6** in DMF are shown in Figure 6.

Relative to $[Fe_4S_4(SPh)_4]^{2-}$, introduction of a π-electron releasing ring substituent is expected to shift the well-defined RS → core charge-transfer absorptions in the visible region to lower energies and displace 2−/3− and 3−/4− potentials to more negative values. This spectral effect was first observed with $[Fe_4S_4(SC_6H_4\text{-}p\text{-}OMe)_4]^{2-}$.[31] All clusters in Table V except those with o-X = OH (**3**) and SMe (**6**) exhibit both these effects. In particular, the visible band (λ_{max} 499 nm) and potentials of $[Fe_4S_4(SC_6H_4\text{-}p\text{-}NH_2)_4]^{2-}$ show the largest shifts of any arenethiolate cluster $[Fe_4S_4(SAr)_4]^{2-}$ yet isolated.[48] Of the clusters **3** and **6** the former exhibits the more pronounced departure from this behavior. Its visible band is blue-shifted by 17 and 37 nm, and the potential of its chemically reversible 2−/3− couple ($i_{p,c}/i_{p,a} \simeq 1$) is anodically shifted by 0.15 and 0.24 V, compared to $[Fe_4S_4(SPh)_4]^{2-}$ and $[Fe_4S_4(SC_6H_4\text{-}p\text{-}OH)_4]^{2-}$, respectively. ^1H NMR spectra of cluster **3** in acetonitrile at 248–298 K revealed no inequivalence of o-C_6H_4OH substituents nor any clear evidence of a fluxional process involving –OH groups. Chemical shifts at ~298 K are given in the Experimental Section for this and other clusters. The –OH signal assignment for **3** was established by deuteration.

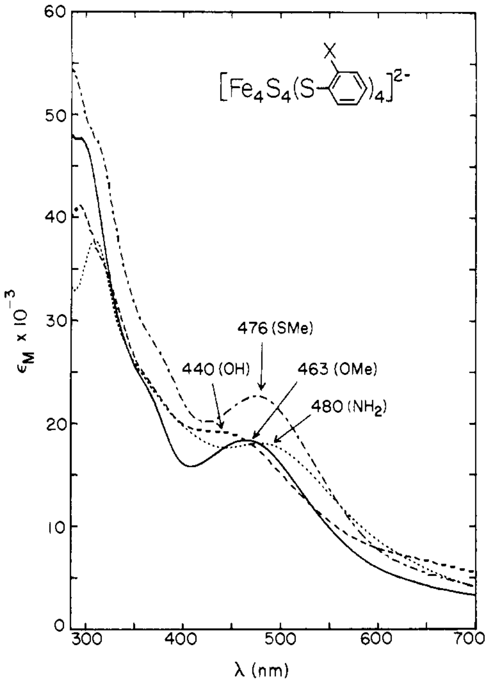

Figure 6. Absorption spectra of $[Fe_4S_4(SC_6H_4\text{-}o\text{-}X)_4]^{2-}$ (X = OH, NH_2, OMe, SMe) in DMF solution. Visible band maxima are given.

The spectral and potential shifts of **3** are in the same direction as those found with other type **1** clusters upon passage from aprotic to protic media.[37] In protic solvents hydrogen bonding to core and terminal sulfur atoms can reasonably account for the direction of these shifts. Such hydrogen-bonding interactions involving core and cysteinate sulfur atoms have been established from X-ray data for $Fe_4S_4(S\text{-}Cys)_4$ sites in proteins.[49] Two types of O··S distances in cluster **3** are listed in Table III: the two shortest distances from each uncoordinated atom O(2–4) to core sulfur atoms, and the four intraligand distances. Taking as an upper limit the ~3.7 Å N··S separation of crystallographically identified (nonlinear)

---

(46) (a) Frankel, R. B.; Averill, B. A.; Holm, R. H. *J. Phys. (Paris)* **1974**, *35*, C6-107. (b) Holm, R. H.; Averill, B. A.; Herskovitz, T.; Frankel, R. B.; Gray, H. B.; Siiman, O.; Grunthaner, F. J. *J. Am. Chem. Soc.* **1974**, *96*, 2644.

(47) Mayerle, J. J.; Denmark, S. E.; DePamphilis, B. V.; Ibers, J. A.; Holm, R. H. *J. Am. Chem. Soc.* **1975**, *97*, 1032.

(48) Consistent with the spectral shift is the observation that $[Fe_4S_4(SC_6H_4\text{-}p\text{-}NMe_2)_4]^{2-}$, the chromophore presumably formed by core extrusion of clostridial ferredoxin with p-$Me_2NC_6H_4SH$, has λ_{max} 535 nm in 80% HMPA/H_2O: Averill, B. A.; Orme-Johnson, W. H. *J. Am. Chem. Soc.* **1978**, *100*, 3034. A compound containing this cluster has not been isolated.

(49) Adman, E.; Watenpaugh, K. D.; Jensen, L. H. *Proc. Natl. Acad. Sci. U.S.A.* **1975**, *72*, 4854.

N–H··S hydrogen bonds in Fe–S proteins,[49] the two shortest distances (3.79, 3.92 Å) of the first type are somewhat long for anything other than incipient hydrogen bonds. Of course, the overall conformation of **3** (Figure 2) may not persist in solution, but further consideration of ligand orientations leads to the conclusion that O–H··S(core) hydrogen bond formation is not favorable. Much more likely is the intraligand hydrogen-bonding interaction **8**, promoted by the necessarily shorter O···S distances of the second type and the partial negative charge on the thiolate sulfur atom. Retention of anodically shifted potentials and the visible feature at ~440 nm (sh) in acetonitrile, a less effective hydrogen bond acceptor than DMF, suggests that the properties of **3** are not strongly influenced by ligand–solvent hydrogen bonding.[50]

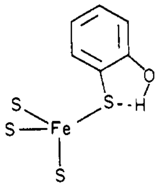

8

It is clear that secondary bonding interactions of the sort present in **3** in the solid are largely absent in acetonitrile solution at 4.2–80 K. As seen in Figure 5b the Mössbauer spectrum of this cluster is dominated by a single quadrupole doublet A with normal parameters (Table IV) for four indistinguishable FeS_4 sites. Just discernible in this spectrum is a high velocity absorption which, by spectral fitting, is associated with a doublet d of a minority component (~7%). Derived parameters of this doublet (δ = 0.55 mm/s, ΔE_Q = 1.62 mm/s) suggest the presence of a Fe(II) impurity or one or more species with secondary bonding interactions.

Summary and Conclusions

The structure of $[Fe_4S_4(SC_6H_4\text{-}o\text{-}OH)_4]^{2-}$ as its crystalline Et_4N^+ salt demonstrates the feasibility of five-coordinate Fe atoms with physiological-type ligands in $[Fe_4S_4]^{2+}$ cores of protein and appropriately constructed synthetic clusters. In cluster **3** one atom, Fe(1), is in a distorted TBP site (structural feature (viii)) with a Fe(1)–O(1)H bond distance some 0.45 Å longer than the Fe–OPh bonds in $[Fe_4S_4(OPh)_4]^{2-}$. Because of this and other aspects of feature vii the Fe(1)–O(1) interaction is termed secondary and, although weak, it exerts an influence on certain bond distance and volume properties of the cluster (features i, iii, and iv). Given the virtually complete absence, by the Mössbauer spectral criterion (Figure 5b), of Fe–OH interactions in frozen acetonitrile solution, it is highly probable that these interactions are imposed properties of the crystalline form of the particular salt of the cluster. This is unlikely to be the case for cluster **7**, which contains two ligands of normally strong chelating tendency. Both Fe–S bonds of the chelate rings are best regarded as primary interactions despite the 0.12-Å difference in bond lengths. As noted,[22] bond length inequalities of comparable extent are not infrequent in chelate complexes of 1,1′-dithio ligands with transition elements.

Intraligand hydrogen-bonding interactions (**8**) are considered to be the most likely cause of the high-energy shift of the visible CT band and anodic potential displacements of cluster **3** in DMF and acetonitrile solutions. This is the initial example of these effects in a solvent medium not containing a protic component.

In addition to the structural proof of four- and five-coordinate Fe sites in a 3:1 distribution in cluster **3**, the present results also show that isomer shifts can be increased by 0.15–0.20 mm/s (4.2 K) as a (presumed) consequence of five-coordination. In cluster **7**, where the higher velocity doublet has been assigned to the five-coordinate sites,[22] the effect is even larger (+0.35 mm/s, Table IV). The P clusters of FeMo proteins of nitrogenase exhibit a 3:1 distribution of sites D and Fe^{2+} in their spin-coupled diamagnetic oxidation level.[17a,c] Mössbauer parameters for the *A. vinelandii* protein are listed in Table IV; those for a clostridial protein are similar, with δ = 0.52 mm/s for both sites.[17c] From comparison with the data for doublet C of **3** and doublet B of **6** it is evident that *isomer shifts very similar to those of P clusters can be achieved without core reduction below the 2+ level.* These shifts and that of **7** are the largest known values for synthetic $[Fe_4S_4]^{2+}$ clusters. The alternative diamagnetic core is fully reduced $[Fe_4S_4]^0$, clusters containing which are produced at extremely negative potentials[7,28,29,36] (Table V). This core has been isolated only in the form of its nonphysiological carbonyl derivative $Fe_4S_4(CO)_{12}$.[51]

Although it has a 3:1 Fe site structure distribution, cluster **3** in its entirety is not a P-cluster model. The quadrupole doublets (A, B) whose ΔE_Q values are closer to that of the three D sites have isomer shifts that are ~0.2 mm/s too low, and the doublet (C) that has a comparable δ value also has a splitting ~1.2 mm/s less than that of the Fe^{2+} site. Thus while secondary interactions by –OH (**3**) and –SMe (**6**) groups (possible simulators of bonding by Tyr and Met side chains, respectively) can raise isomer shifts very close to those of P clusters, they have not afforded the ΔE_Q ~3 mm/s value of the Fe^{2+} site—at least not in the geometries and core oxidation level encountered here. The latter site has been interpreted in terms of a tetrahedral $Fe(II)S_4$ unit.[17a,c] Phenoxide ligands in the tetrahedral FeS_3O sites of $[Fe_4S_4(OPh)_4]^{2-}$ (Table IV) increase δ values by ~0.05 mm/s compared to type **1** clusters and do not afford an exceptional increase in quadrupole splitting. Given that the imposition of five-coordination is at present the only known means of increasing isomer shifts of the $[Fe_4S_4]^{2+}$ core to values close to those of diamagnetic P clusters, this structural feature merits inclusion in formulations, and in approaches to synthetic representations, of these clusters. A reasonable objective would appear to be a cluster with three five-coordinate sites ligated such as to bias charge distribution toward Fe(II) in the fourth, FeS_4-type site. Choice of other clusters as synthetic targets would of course depend on the acceptance of the 2+ core and the interpretation of the protein Fe^{2+} site. In addition to reasonable agreement with Mössbauer spectral parameters, another necessary feature of any P-cluster model is a one-electron oxidation to an EPR-silent ($S \geq {}^5/_2$) form.[17] Synthetic investigations relevant to the P-cluster problem are continuing.

Acknowledgment. This research was supported by NIH Grant GM 28856 at Harvard University and by a grant from the National Science Foundation to the Francis Bitter National Magnet Laboratory at MIT. NMR and X-ray diffraction equipment used in this research were obtained by NSF Grants CHE 80-00670 and CHE 80-08891. We thank J. M. Berg for volume calculations, Dr. J.-J. Girerd for experimental assistance, and Prof. B. A. Averill for a preprint of ref 21b.

Registry No. 3, 87614-71-9; **4**, 87614-73-1; **5**, 87614-75-3; **6**, 87614-77-5; $[Fe_4S_4(SC_6H_4\text{-}p\text{-}OH)_4]^{2-}$, 87614-78-6; $[Fe_4S_4(SC_6H_4\text{-}p\text{-}OMe)_4]^{2-}$, 87614-79-7; $[Fe_4S_4(SC_6H_4\text{-}p\text{-}NH_2)_4]^{2-}$, 87614-80-0; $[Fe_4S_4(SPh)_4]^{2-}$, 52325-39-0; $(Et_4N)_2[Fe_4S_4(S\text{-}t\text{-}Bu)_4]$, 62873-87-4; $(n\text{-}Bu_4N)_2[Fe_4S_4(S\text{-}t\text{-}Bu)_4]$, 50923-25-6; $HOC_6H_4\text{-}o\text{-}SH$, 1121-24-0; $H_2NC_6H_4\text{-}o\text{-}SH$, 137-07-5; $MeOC_6H_4\text{-}o\text{-}SH$, 7217-59-6; $MeSC_6H_4\text{-}o\text{-}SH$, 54615-64-4.

Supplementary Material Available: X-ray structural data for $(Et_4N)_2[Fe_4S_4(SC_6H_4\text{-}o\text{-}OH)_4]$— atom coordinates of cations, anisotropic temperature factors, calculated hydrogen positions and temperature factors, and tabulations of $10|F_o|$ and $10|F_c|$ (27 pages). Ordering information is given on any current masthead page.

---

(50) The possibility that the properties of **3** in solution are influenced by linkage isomerism, i.e., $Fe\text{-}SC_6H_4\text{-}o\text{-}OH \rightarrow Fe\text{-}OC_6H_4\text{-}o\text{-}SH$, appears to be most unlikely because $[Fe_4S_4(OPh)_4]^{2-}$ is nearly completely converted to $[Fe_4S_4(SPh)_4]^{2-}$ by 4 equiv of PhSH in acetonitrile solution.[21b]

(51) Nelson, L. L.; Lo, F. Y.-K.; Rae, A. D.; Dahl, L. F. *J. Organomet. Chem.* **1982**, *225*, 309.